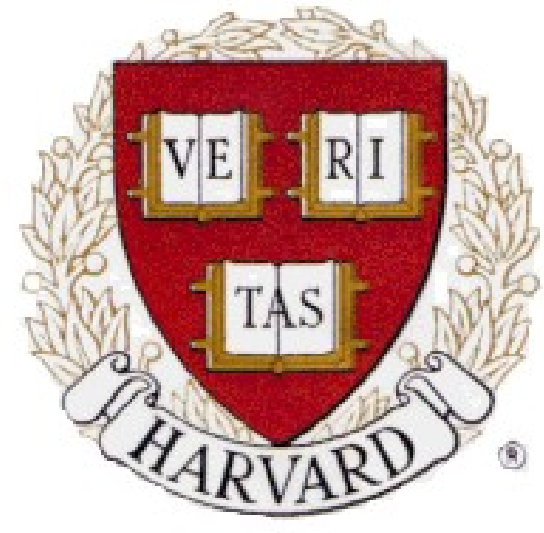


# New Measurement of the Electron Magnetic Moment and Fine Structure Constant



D. Hanneke, B. Odom, B. D'Urso, G. Gabrielse  
Department of Physics, Harvard University, Cambridge, MA 02138, USA



$$g/2 = 1.001\,159\,652\,180\,85\,(76) [0.76 \text{ ppt}]$$

$$\alpha^{-1} = 137.035\,999\,710\,(96) [0.70 \text{ ppb}]$$

## The g-value

### Magnetic Moment

Orbital angular momentum  $g$  depends on the relative distribution of charge and mass.  
 $g = 1$  applies for an identical distribution.

$$\mu = -g \frac{e\hbar}{2m} \frac{S}{\hbar}$$

### Electron Structure

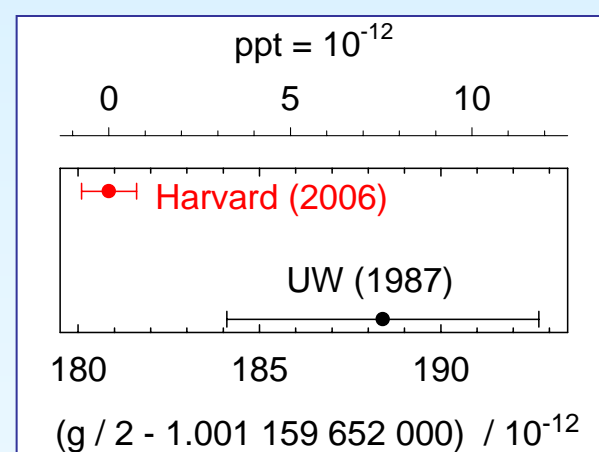
Deviations of the measured  $g$  from that predicted by QED could indicate the presence of constituents of the electron with characteristic mass ( $m$ ) that goes as<sup>5</sup>

$$\left| \frac{\delta g}{2} \right| \approx \left( \frac{m}{m_e} \right)^2$$

Using values of the fine structure constant from either the Rb<sup>4</sup> or Cs<sup>5</sup> measurements gives a value of  $|\delta g/2| < 1.5 \times 10^{-12}$ , which sets a limit of  $m > 130 \text{ GeV}/c^2$ . This corresponds to a limit on the electron radius of  $R < 1 \times 10^{-16} \text{ m}$ . For comparison, the largest  $e/e^+$  collider (LEP) probes for a contact interaction at 10.3 TeV<sup>12</sup>.

Dirac point particle  
 $g = 2$

Interactions with the QED vacuum  
 $g = 2.002\,319\,304\dots$



Measurements using a single-electron quantum cyclotron yield a new value for the electron magnetic moment, the  $g$ -value, at the 0.76 ppt level<sup>1</sup>, nearly six times more accurate than previous measurements<sup>2</sup>. When coupled with a quantum electrodynamics (QED) calculation, the new measurements determine the fine structure constant,  $\alpha$ , at the 0.70 ppb level<sup>3</sup>, ten times more accurate than atom-recoil determinations<sup>4,5</sup>. Comparisons of these independent measurements of  $\alpha$  provide the most stringent test of QED theory. Given a model for internal electron structure<sup>6</sup>, these comparisons set a limit on any such substructure at the 130 GeV scale - quite large, given that we carry out the experiment at 100 mK.

The high precision of our measurement arises from the combination of many useful techniques. A single-electron quantum cyclotron<sup>7</sup>, so-called because we use a quantum non-demolition measurement to resolve the lowest cyclotron and spin levels, is held in a cylindrical Penning trap<sup>8</sup>, whose well-understood cavity-mode structure<sup>9</sup> is used to inhibit spontaneous emission<sup>10</sup> and to set limits on shifts from electron-cavity coupling. Our low temperature (100 mK) narrows the linewidths of the measured frequencies and inhibits stimulated absorption in the cyclotron motion, effectively locking it in the ground state. A self-excited oscillator increases the signal-to-noise<sup>11</sup>.

Further investigations into the electron-cavity coupling and the lineshapes of the measured frequencies, as well as a new apparatus designed for high stability, promise additional increases in accuracy.

## The Fine Structure Constant

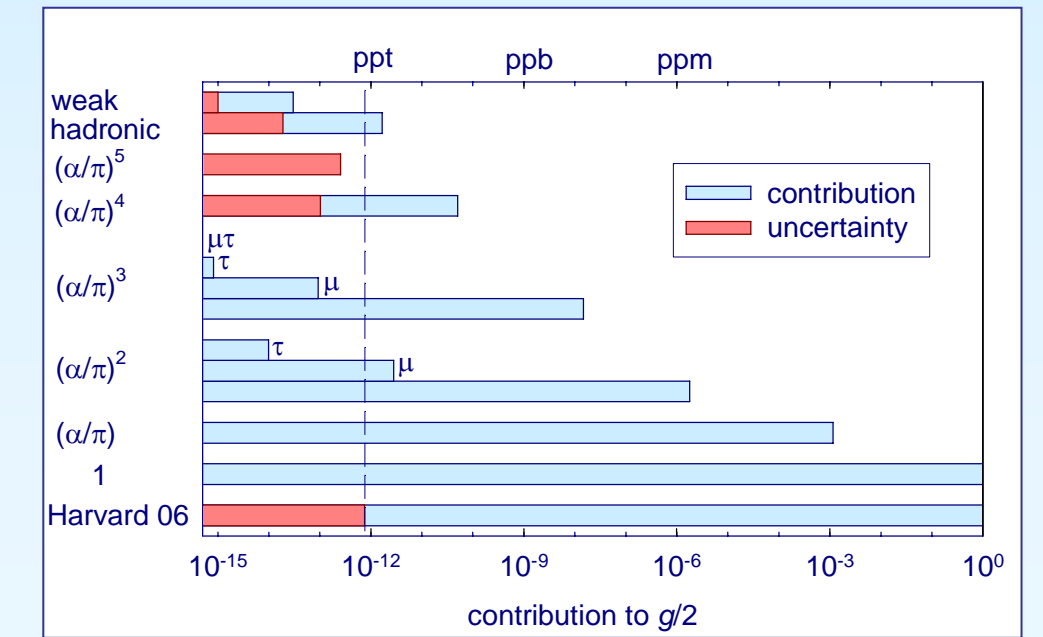
$$\frac{g}{2} = 1 + C_2 \left( \frac{\alpha}{\pi} \right) + C_4 \left( \frac{\alpha}{\pi} \right)^2 + C_6 \left( \frac{\alpha}{\pi} \right)^3 + C_8 \left( \frac{\alpha}{\pi} \right)^4 + \dots + a_{\mu\tau} + a_{\text{hadronic}} + a_{\text{weak}}$$

In Quantum Electrodynamics, the  $g$ -factor can be written as an expansion in powers of the fine structure constant. Contributions from hadronic and weak vacuum polarizations are much smaller and well understood.

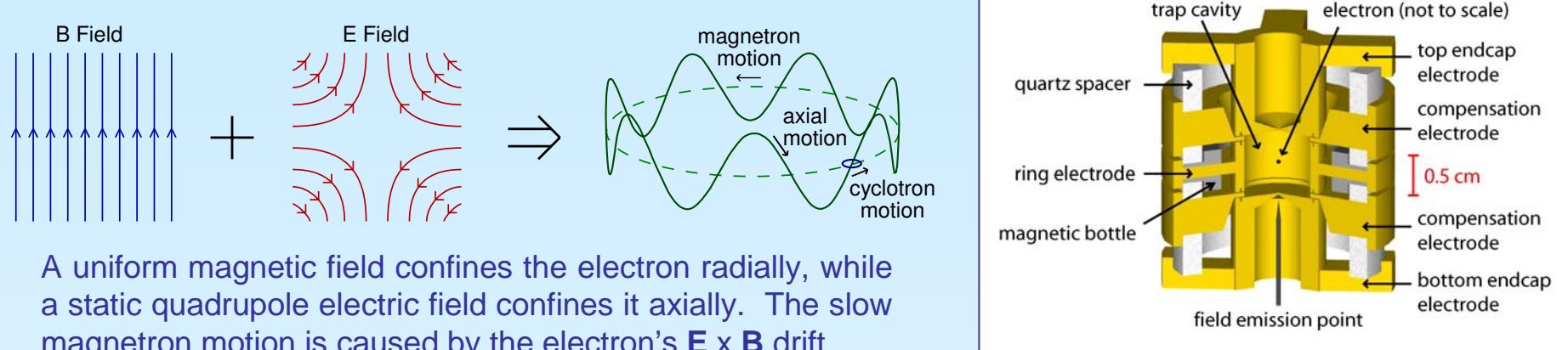
$$\alpha = \frac{1}{4\pi\epsilon_0} \frac{e^2}{\hbar c}$$

By inverting the series, we use our measurement of the  $g$ -factor to obtain a value of the fine structure constant that is a factor of ten less uncertain than the next-best determinations.

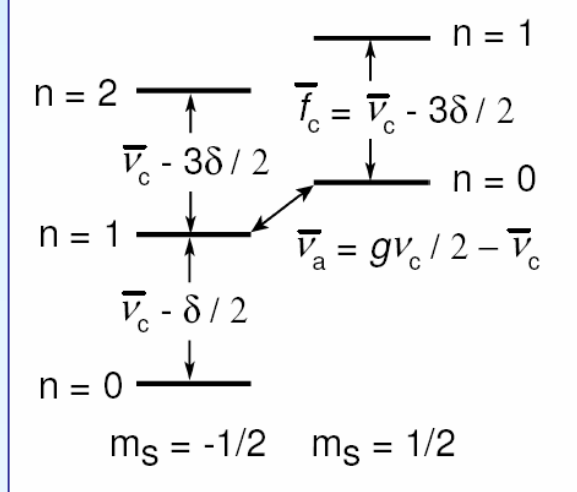
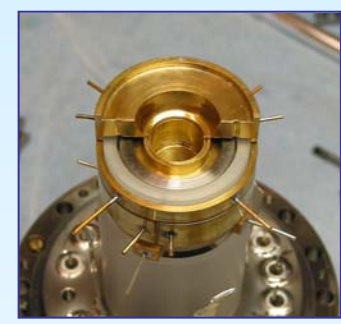
The theoretical uncertainty, due primarily to an estimate of  $C_6$  and the calculation of  $C_8$  (the prior coefficients are known exactly), is nearly a factor of three lower than our experimental uncertainty.



## The Penning Trap

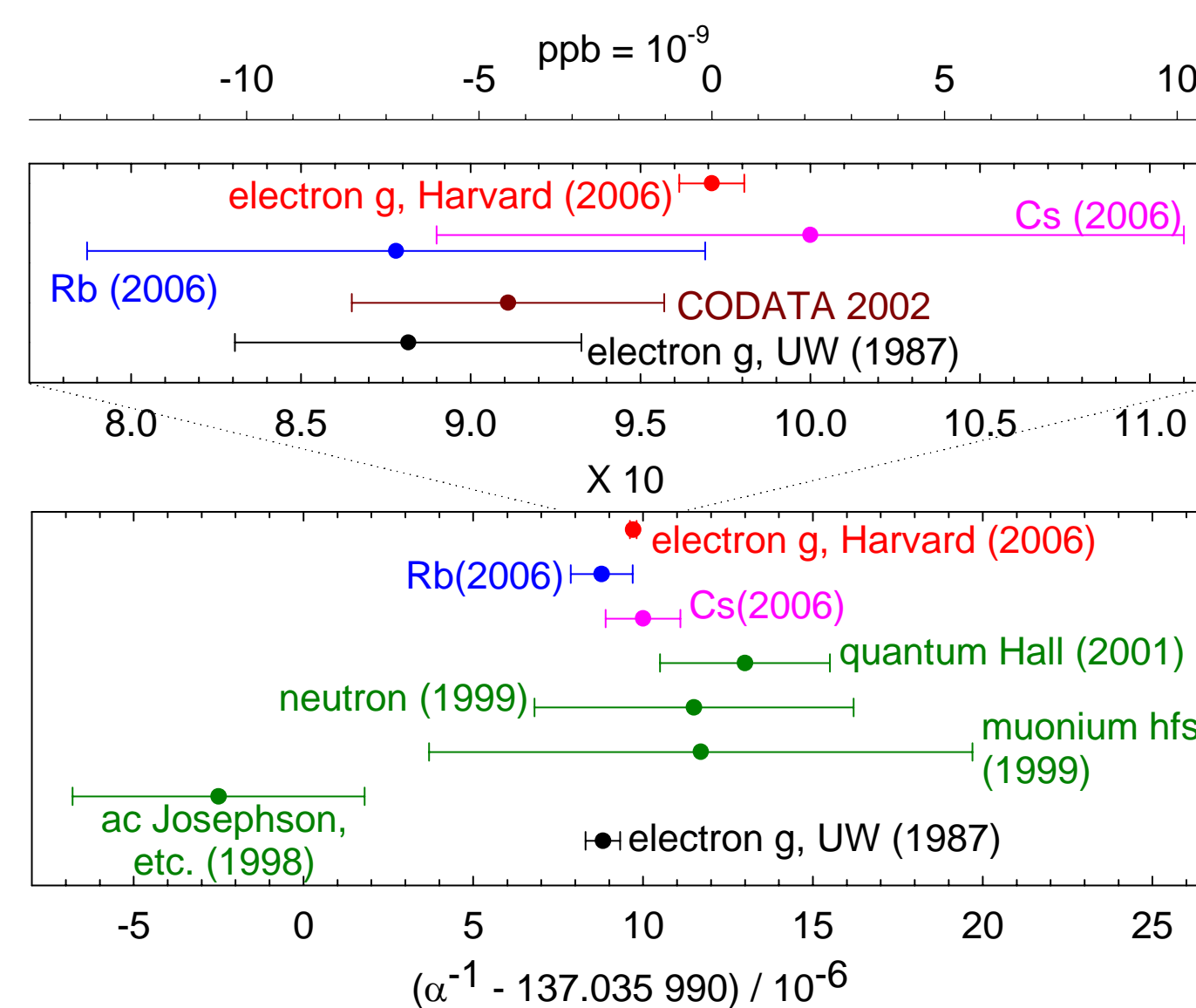


motion	frequency	$h\nu/k_B$	damping
axial	200 MHz	10.0 mK	1 Hz
cyclotron	149.0 GHz	7.2 K	0.02 Hz
spin	149.2 GHz	7.2 K	$10^{-10}$ Hz
magnetron	134 kHz	0.64 $\mu$ K	$10^{-10}$ Hz

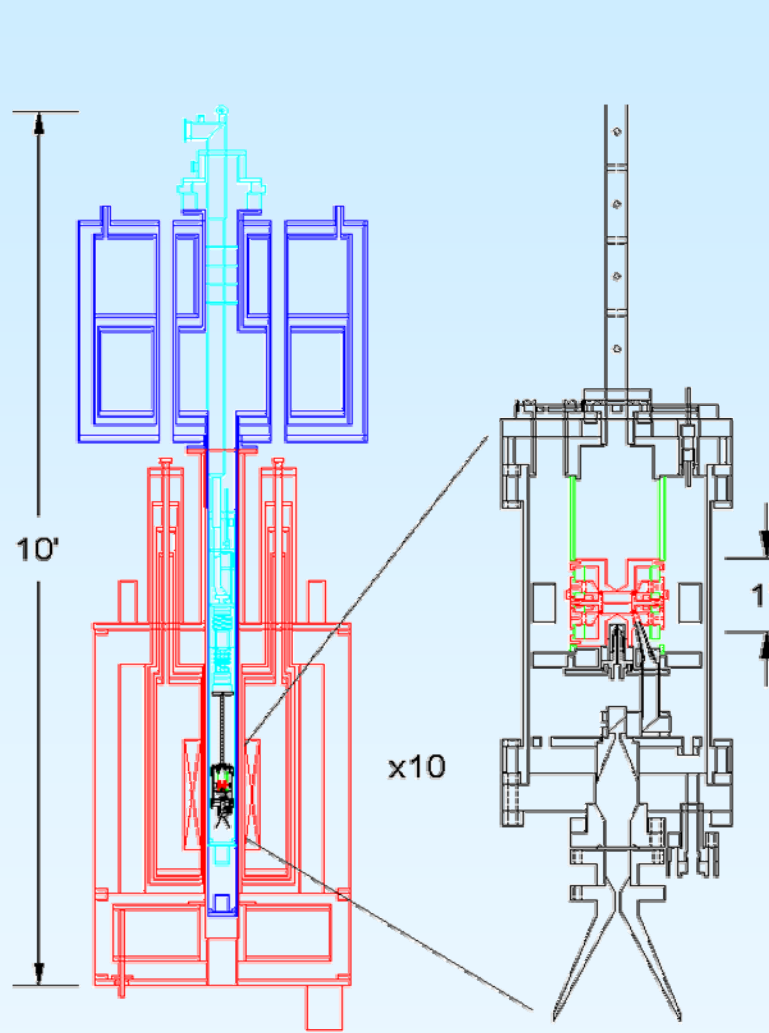
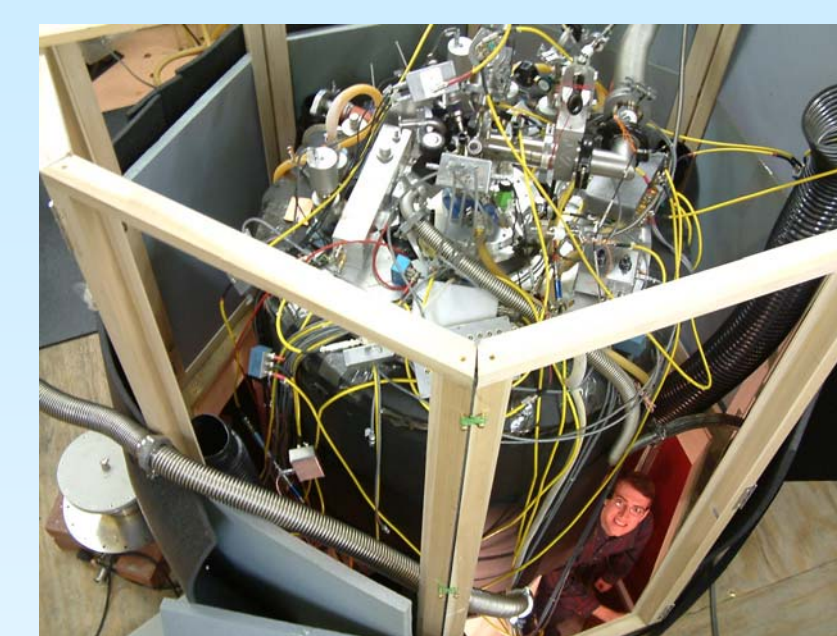


$$\frac{g}{2} = \frac{\bar{\nu}_c + \bar{\nu}_a}{\nu_c} \approx 1 + \frac{\bar{\nu}_a - \bar{\nu}_c^2 / (2\bar{\nu}_c)}{\bar{\nu}_c + 3\delta/2 + \bar{\nu}_c^2 / (2\bar{\nu}_c)}$$

In free space, the  $g$ -factor is just twice the ratio of the spin to the cyclotron frequency, but in a Penning trap, the electric field perturbs the magnetic motion, resulting in a correction to the measured anomaly and cyclotron frequencies. The Brown-Gabrielse invariance theorem relates the free-space cyclotron frequency to the measured eigenfrequencies of a trap (even a slightly misaligned one). There is also a relativistic correction  $\delta$ , which is approximately  $10^9$  times the cyclotron frequency.



## The Apparatus

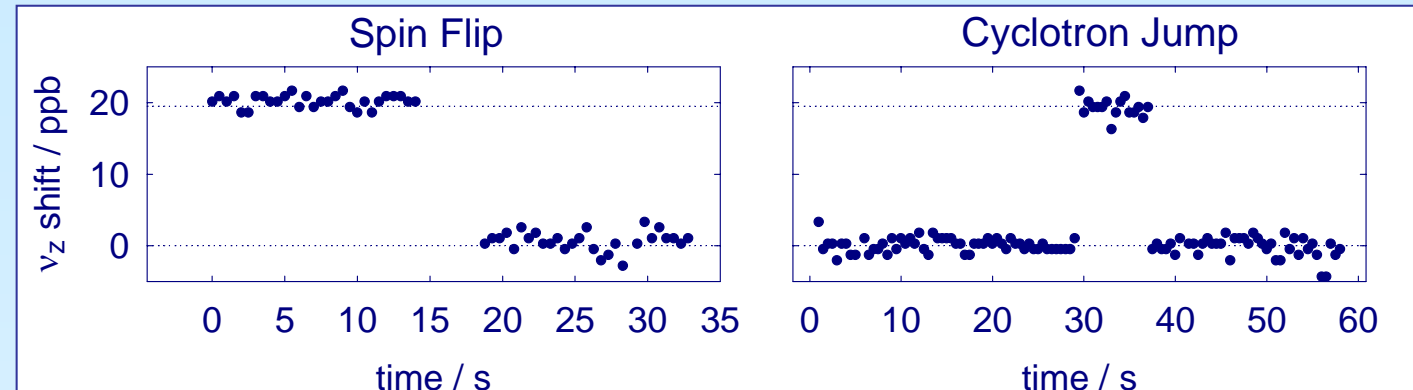


A 5.3 T superconducting solenoid provides the field for the Penning trap. A dilution refrigerator cools the trap electrodes to 100 mK. The trap electrodes are made out of silver and the vacuum enclosure out of titanium to avoid the temperature-dependent nuclear paramagnetism of copper. It is a tabletop experiment...provided you have a high enough ceiling.

## The Quantum Cyclotron

### Axial Detection

The electron's axial motion induces image currents on the trap electrodes. By coupling these currents to a tuned circuit and increasing them with cold single-FET amplifiers, we can measure the frequency and relative amplitude of this motion. By positively feeding the detected signal back to the electron (a self-excited oscillator), we greatly increase our signal-to-noise and can measure the axial frequency to better than 1 Hz in 200 MHz.

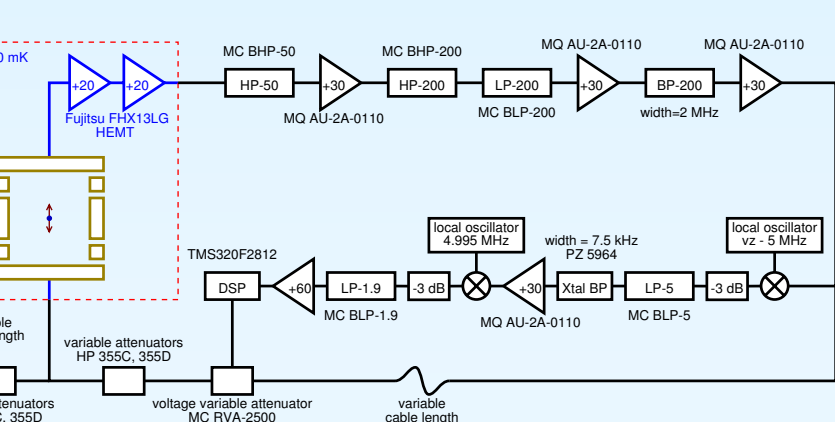
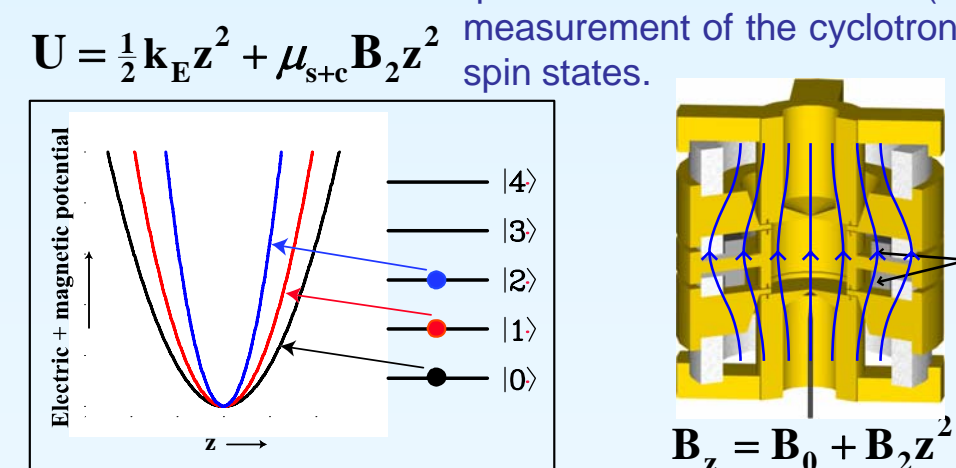


### Low Temperature

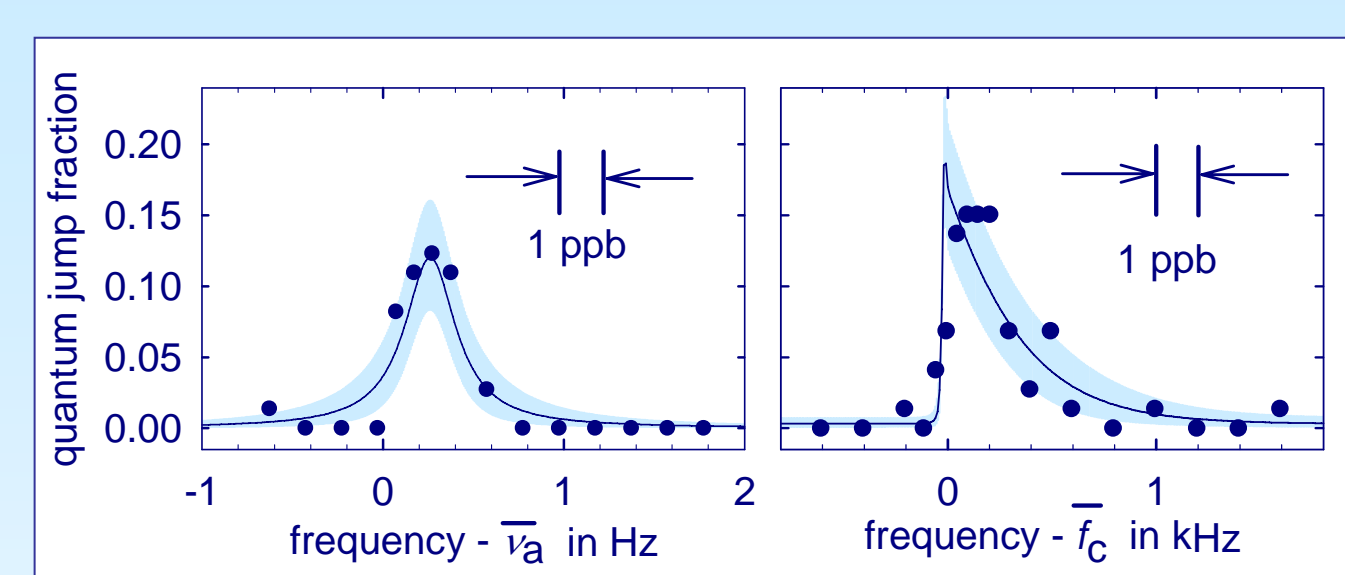
Running at 100 mK inhibits stimulated absorption in the cyclotron motion, effectively locking it in the ground state and allowing single-quantum cyclotron spectroscopy. Using only the lowest quantum levels allows us to account for the relativistic shift (approximately 1 ppb/quantum), which broadens the line in classical spectroscopy. Since the cyclotron and axial motions are coupled through the magnetic bottle, the lower axial temperature narrows the linewidths of the cyclotron and anomaly frequencies.

### Cyclotron Detection

The 149 GHz cyclotron frequency is too high for direct detection, so we couple it to the axial motion through a quadratic perturbation in the magnetic field. The perturbation (the "magnetic bottle") is established with a pair of saturated nickel rings and makes the depth of the axial potential well depend on the total magnetic moment of the electron and thus on the spin and cyclotron states. For our bottle, a quantum jump corresponds to a 4 Hz shift (20 ppb) in axial frequency. Monitoring the axial frequency is a quantum non-demolition (QND) measurement of the cyclotron and spin states.



## Measurement & Uncertainty



Applied corrections and uncertainties in $g$ in ppt.		
Source	146.8 GHz	149.0 GHz
$\nu_s$ shift	0.2(0.3)	0.00(0.02)
Anomaly power	0.0(0.4)	0.00(0.14)
Cyclotron power	0.0(0.3)	0.00(0.12)
Cavity shift	12.8(5.1)	0.06(0.39)
Lineshape model	0.0(0.6)	0.00(0.60)
Statistics	0.0(0.2)	0.00(0.17)
<b>Total (in ppt)</b>	<b>13.0(5.2)</b>	<b>0.06(0.76)</b>

### Anomaly Procedure

- With the electron in the  $|n=0, m_s = 1/2\rangle$  state, pulse the anomaly drive (173 MHz).
- Look for a transition to  $|1, -1/2\rangle$ , which decays to  $|0, -1/2\rangle$ .
- Make a histogram of spin flips versus frequency.
- Prepare for the next measurement by putting the electron back into the  $|0, 1/2\rangle$  state using a simultaneous cyclotron and anomaly drive.

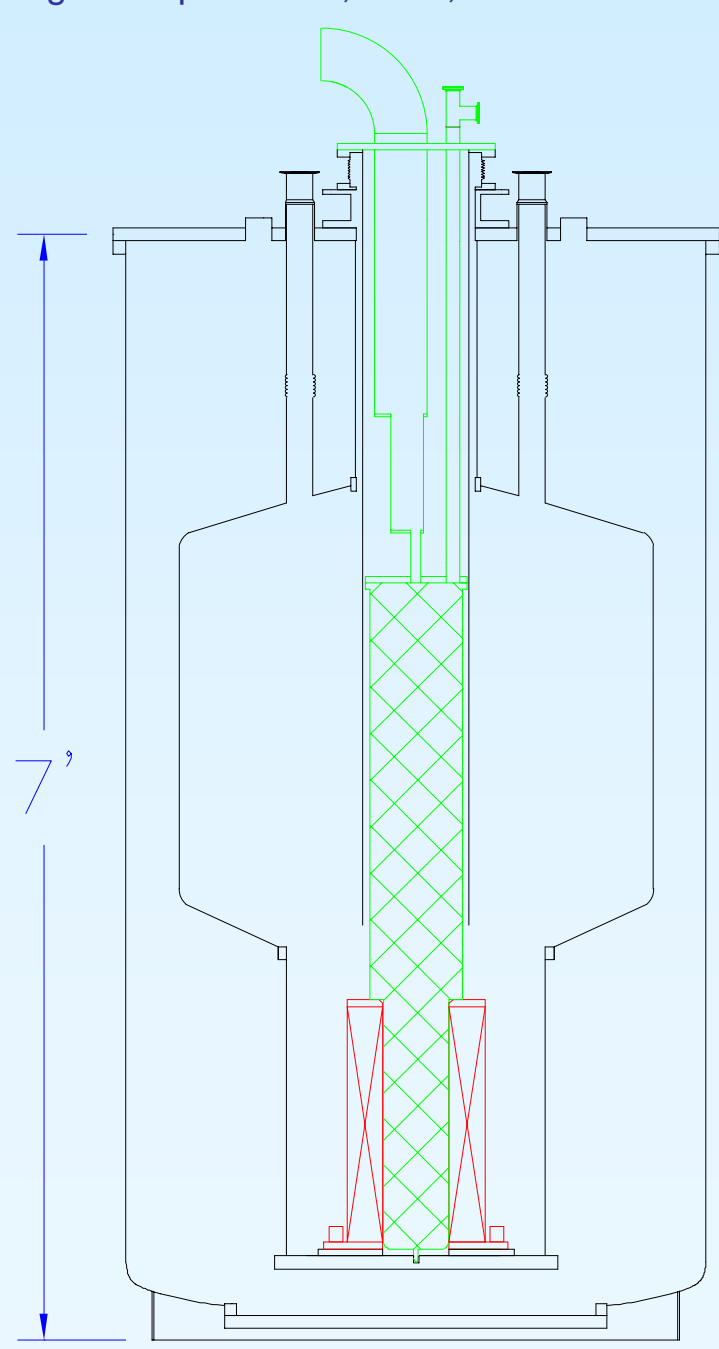
### Cyclotron Procedure

- With the electron in the  $|n=0, m_s = 1/2\rangle$  state, pulse the cyclotron drive (149.0 GHz).
- Look for excitations to  $n \geq 1$ .
- Make a histogram of excitations versus frequency.

## The Future

### Next-Generation Apparatus

Currently under construction is a next-generation apparatus, designed to achieve the utmost stability of magnetic field. The refrigerator will sit directly on the magnet form, eliminating any shifts due to temperature and pressure fluctuations as well as reducing vibration effects. The magnet is designed to minimize drift in persistent mode, and the cryogen reservoir will be large, with regulated pressures, flows, and level around the refrigerator.



### Cyclotron Damping Maps

Since the spontaneous emission rate of a cyclotron excited state depends on its proximity to a cavity mode, we can use this rate to map the mode locations. While creating such a map would be considerably slower than the synchronized cloud technique, the result would reveal the exact coupling experienced by a single electron and eliminate extra modes seen when using an extended cloud. It has the potential to better reveal the mode location and Q's.

### Axial Sideband Cooling

By decoupling the axial motion from the amplifiers, we can use an axial sideband of the cyclotron frequency to cool the axial state. Since the magnetic bottle couples the width of the cyclotron and anomaly lines to the axial energy, axial sideband cooling can greatly narrow our linewidths.

## Spin-offs

- CPT test by comparing  $g_{e-}$  and  $g_{e+}$
- Tests of Lorentz invariance by searching for sidereal variations in the anomaly frequency
- Proton magnetic moment
- Proton-electron mass ratio

## Cavity Effects

### Inhibited Spontaneous Emission

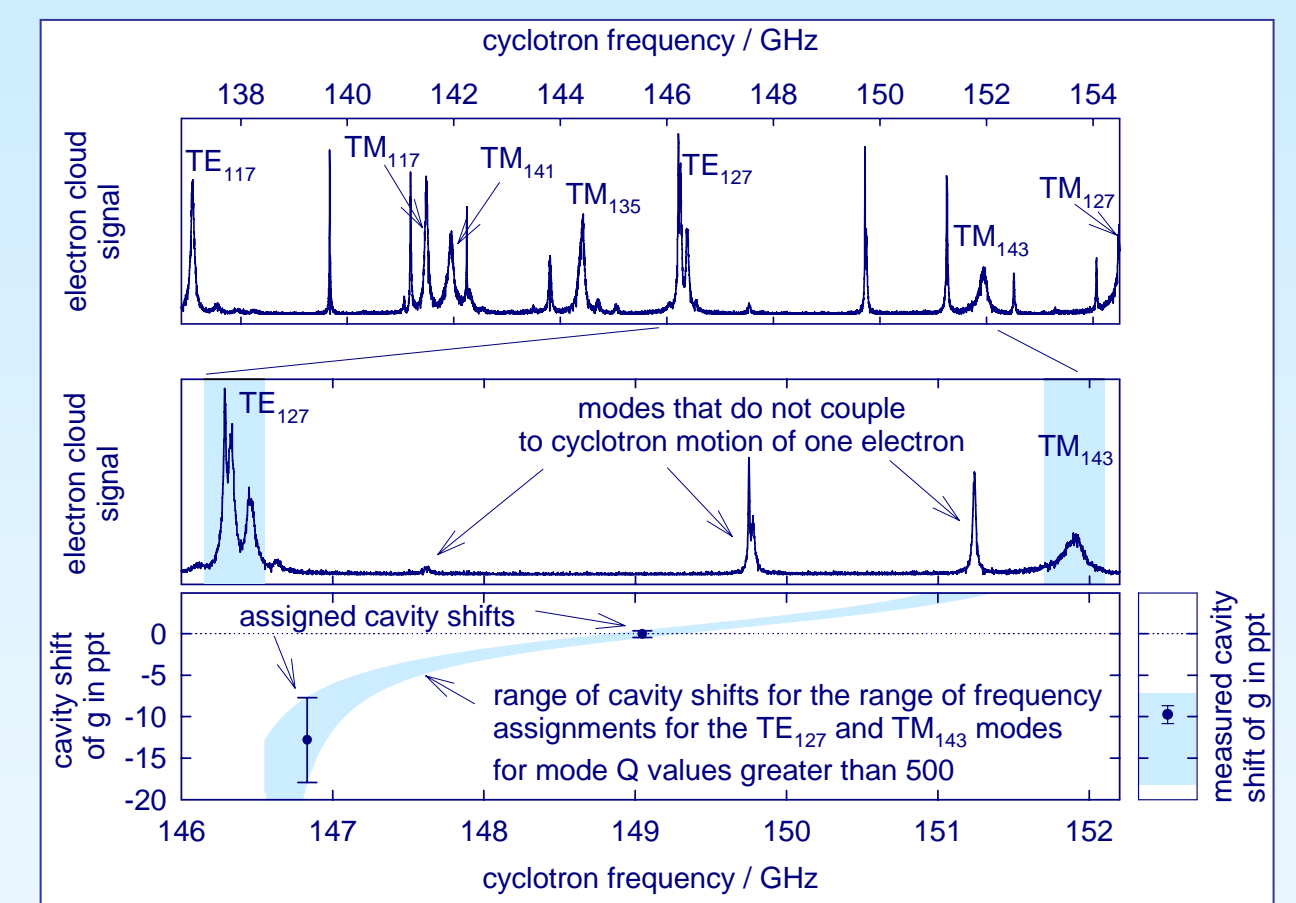
The trap electrodes form a high-Q microwave cavity with resonant modes near the cyclotron frequency. The cyclotron motion couples to modes that have a transverse electric field at the trap center. Since transition rates are proportional to the density of the final states, tuning the cyclotron frequency between two modes inhibits the spontaneous emission rate. For example, at 149.0 GHz the lifetime of an excited cyclotron state is 6.7 s, a factor of nearly 70 above the free-space lifetime of 100 ms.

### Frequency Shifts

The cavity modes and the cyclotron degree of freedom are coupled oscillators that pull each other's frequencies. Since the cyclotron frequency is essentially half of a  $g$ -value measurement, this cavity shift is an important systematic error. The plot shows the first measured cavity shift of  $g$  and the calculated shifts based on the location of the modes in our cavity.

### Measuring Mode Locations

We measure the cavity modes (e.g. the top figure) using a cloud of several hundred to thousands of electrons, driven parametrically. When the electrons' cyclotron frequency is resonant with a cavity mode, their axial motion synchronizes. Since the cloud has a non-zero spatial extent, this method detects some modes that do not couple to a single electron.



## References

- B. Odom, D. Hanneke, B. D'Urso, and G. Gabrielse, to be published (2006).
- R. S. Van Dyck, Jr., P. B. Schwinberg, and H. G. Dehmelt, Phys. Rev. Lett. **59**, 26 (1987).
- G. Gabrielse, D. Hanneke, T. Kinoshita, M. Nio, and B. Odom, to be published (2006).
- P. Cladé, E. de Mirandes, M. Cadoret, S. Guellati-Khélifa, C. Schwob, F. Nez, L. Julien, and F. Biraben, Phys. Rev. Lett. **96**, 033001 (2006).
- V. Gerginov, K. Calkins, C. E. Tanner, J. McFerran, S. Diddams, A. Bartels, and L. Hollberg, Phys. Rev. A **73**, 032504 (2006).
- S. J. Brodsky and S. D. Drell, Phys. Rev. D **22**, 2236 (1980).
- S. Peil and G. Gabrielse, Phys. Rev. Lett. **83**, 1287 (1999).
- G. Gabrielse and F. C. MacKintosh, Intl. J. of Mass Spec. and Ion Proc. **57**, 1 (1984).
- L. S. Brown and G. Gabrielse, Rev. Mod. Phys. **58**, 233 (1986).
- G. Gabrielse and H. Dehmelt, Phys. Rev. Lett. **55**, 67 (1985).
- B. D'Urso, R. Van Handel, B. Odom, D. Hanneke, and G. Gabrielse, Phys. Rev. Lett. **94**, 113002 (2005).
- D. Bourilov, Phys. Rev. D **64**, 071701R (2001).